Test of the Hemisphere Rule of Magnetic Twist in Solar Active Regions Using the Helioseismic and Magnetic Imager (HMI) Vector Magnetic Field Data

Y. Liu[1], J. T. Hoeksema[1], X. Sun[1]

ABSTRACT

Magnetic twist in solar active regions has been found to have a hemispheric preference in sign (hemisphere rule): negative in the northern hemisphere and positive in the southern. The preference reported in previous studies ranges greatly, from $\sim 58\%$ to 82%. In this study, we examine this hemispheric preference using vector magnetic field data taken by HMI and find that $75\% \pm 7\%$ of 151 active regions studied obey the hemisphere rule, well within the preference range in previous studies. If the sample is divided into two groups – active regions having magnetic twist and writhe of the same sign and having opposite signs – the strength of the hemispheric preference differs substantially: $64\% \pm 11\%$ for the former group and $87\% \pm 8\%$ for the latter. This difference becomes even more significant in a sub-sample of 82 active regions having a simple bipole magnetic configuration: $56\% \pm 16\%$ for the active regions having the same signs of twist and writhe, and 93% with lower and upper confidence bounds of 80% and 98% for the active regions having the opposite signs. The error reported here is a 95% confidence interval. This may suggest that, prior to emergence of magnetic tubes, either the sign of twist does not have a hemispheric preference or the twist is relatively weak.

Subject headings: Sun: dynamo—Sun: surface magnetism—Sun: magnetic topology

1. Introduction

Magnetic twist, *the twist of field lines about a central axis*, is an inherent property of the solar magnetic field that provides insight into the physical processes by which a flux tube is generated in the solar interior and evolves during its buoyant rise to the photosphere.

[1]W. W. Hansen Experimental Physics Laboratory, Stanford University, Stanford, CA94305-4085

Flux tubes rising through the convection zone (CZ) are already twisted when they emerge at the solar surface (e.g. Lites et al. 1995; Leka et al. 1996). This implies that the Sun's interior processes generate twist in emerging flux tubes. The direction of the twist has a hemispheric preference: negative twist dominates in the northern hemisphere and positive in the southern. This observed preference is known as the hemispheric helicity rule (hemisphere rule hereafter).

The strength of the preference in various features is observed to be different (e.g. Martin et al. 1994; Pevtsov & Balasubramaniam 2003; Rust & Kumar 1996; Lim & Chae 2009; Pevtsov et al. 1995; Bao & Zhang 1997). It is higher in quiescent filaments ($\sim$82%) and lower in active regions (ARs; $\sim$58 – 82%) on average. Table 1 of Wang (2013) gives a summary of results in previous studies. Wang (2013) argues that difficulty in determining the sign of the twist in newly emerged ARs causes this discrepancy, and the strength of the preference in ARs should indeed be similar to that in quiescent filaments.

A variety of subsurface mechanisms for producing twist in emerging flux tubes have been proposed. These mechanisms can be separated into two groups: those associated with the creation of flux tubes and those acting during their rise. In other words, the twist may originate in the dynamo process at the base of the CZ, or it may be acquired during the tube's rise through the CZ.

The dynamo process can impart twist to flux tubes through both the Ω-effect and the α-effect (e.g. Berger & Ruzmaikin 2000; Kleeorin et al 2003; Nandy 2006; Zhang et al. 2006), the two essential ingredients in standard mean-field dynamo theory. Berger & Ruzmaikin (2000) predict that the differential rotation inherently generates magnetic helicity, of which twist is one component. This Ω-effect produces toroidal magnetic field from the poloidal component and creates "a helical field structure within the Sun with spirals of opposite sign in the northern and southern hemispheres." (Berger & Ruzmaikin 2000).

The α-effect generates a mean electromotive force along the mean magnetic field caused by fluctuating components in the magnetic and velocity fields (Parker 1955). The α-effect creates poloidal magnetic field from toroidal field. This effect is closely related to the kinetic helicity of the turbulence (Krause & Rädler 1980). Simulation and theory indicate that kinetic helicity produces magnetic helicity of the same sign at the basic convective size-scale and an equal amount of helicity of the opposite sign at larger scales (Pouquet et al. 1976; Seehafer 1996; Ruzmaikin 1996). The basic size scale of the energy-carrying eddies in the Sun is about 50 Mm (Brandenburg et al. 2011), roughly the size of a typical active region (AR).

Flux tubes can also acquire twist during their buoyant rise through the CZ. As an Ω-

shaped tube ascends from the bottom of the CZ, the Coriolis force acting on the rising tube tilts one leg of the tube toward the equator and the other away (e.g. D'Silva & Choudhuri 1993; Fan et al. 1993). This deformation generates magnetic writhe, *a measure of the helical distortion of the tube's central axis*. Helicity in a flux tube can be decomposed into twist and writhe. In order to conserve helicity, the same amount of twist is produced within the tube, but with the opposite sign (hereafter called the C-effect).

As a flux tube rises through the CZ it is also buffeted by the turbulence of convection outside of the tube. The convective turbulence has a non-zero kinetic helicity, which causes the tube to deform (Σ-effect; Longcope et al. 1998). This deformation produces magnetic writhe in the tube. Again, to conserve helicity the same amount of magnetic twist of opposite sign must be generated in the tube.

The sign relationship between twist and writhe in a flux tube when it reaches the photosphere may depend upon how much twist the tube initially possesses. If the initial twist in a flux tube is high enough, it leads to a kink instability in the tube, i.e., part of the twist will be converted to writhe. This writhe has the same sign as the twist, as simulations have shown (Linton et al. 1996, 1999). On the other hand, if a flux tube has weak twist or no twist initially, the C-effect and Σ-effect will generate twist by deforming the flux tube during its rising through CZ. This sign of the acquired twist will be opposite to that of the writhe, and is consistent with the hemisphere rule (Longcope et al. 1998; Holder et al. 2004). For this reason, it is interesting to separate ARs into two groups: ARs having the same signs of twist and writhe and ARs having the opposite signs, and examine their hemispheric preferences separately. If these two groups of ARs show different strengths of the hemisphere rule, that might explain the large range of preferences ($\sim$58%$-$82%) reported in previous studies (Seehafer 1990; Pevtsov et al. 1995; Bao & Zhang 1997; Longcope et al. 1998; Hagino & Sakurai 2004; Zhang et al. 2010b; Hao & Zhang 2011; Yang & Zhang 2012). The separation might further shed some light on the origin of magnetic twist in ARs.

In this study, we use the *Helioseismic and Magnetic Imager* (HMI; Scherrer et al. 2012; Schou et al. 2012) vector magnetic field data (Hoeksema et al. 2013) to test the hemisphere rule of magnetic twist in ARs. The paper is organized as follows. Data processing, sample selection and calculation of proxies of twist and writhe are described in Section 2. Section 3 presents results. We summarize and discuss the results of this study in Section 4.

2. Data and Calculations

We use vector magnetic field data taken by HMI for this investigation. The HMI instrument is a filtergraph with full disk coverage at 4096×4096 pixels. The spatial resolution is about 1" with a 0.5" pixel size. The spectral line is the FeI 6173Å absorption line formed in the photosphere (Norton et al. 2006). The Stokes parameters [I, Q, U, V], measured at 6 wavelength positions and sampled every 720 seconds using a 1350 seconds weighted average in order to suppress the p modes and increase the signal-to-noise ratio, are inverted to retrieve the vector magnetic field using a Milne-Eddington based inversion algorithm, Very Fast Inversion of the Stokes Vector (VFISV; Borrero et al. 2010; Centeno et al. 2013). The 180° degree ambiguity of the azimuth is resolved using a "minimum energy" algorithm (Metcalf 1994; Leka et al. 2009). The location and extent of the ARs are automatically identified and bounded by a feature recognition model (Turmon et al. 2010), and the disambiguated vector magnetic field data of ARs are deprojected to heliographic coordinates (Bobra et al. 2013). Here we use Lambert (cylindrical equal area) projection method centered on the region for the remapping.

We select ARs based upon availability of processed HMI vector magnetic field data. We analyzed each NOAA AR when at least 24 hours of vector data are available near central meridian passage. Vector magnetic field measurements near Sun's disk center have less noise. We use 24 hours of observation (usually 120 datasets of vector magnetic field) to reduce errors and minimizes the effects of dramatic evolution of the AR. In total, 151 ARs are analyzed. Distribution of maximum change of magnetic flux for these 151 ARs is shown in Fig. 1. Φ is median of unsigned flux and $\delta\Phi$ is the difference of maximum and minimum of the unsigned fluxes in the 24 hours of observation, respectively. Median of $\delta\Phi/\Phi$ is ∼15%. This indicates that this sample only includes a few ARs that underwent dramatic evolution.

A force-free field satisfies $\bigtriangledown \times \mathbf{B} = \alpha\mathbf{B}$, where $\mathbf{B}$ is magnetic field and α is a scalar quantity that depends on position. The force-free α parameter is usually used as a measure of magnetic twist in an AR (e.g. Seehafer 1990; Pevtsov et al. 1995). We choose a B_z^2 weighted force-free α_w, proposed by Hagino & Sakurai (2004) as a proxy of the twist in the AR. α_w is defined as,

$$\alpha_w = \frac{\int_S \alpha(x,y) B_z^2(x,y) dxdy}{\int_S B_z^2(x,y) dxdy}, \tag{1}$$

where B_z is the vertical component of magnetic field. The integral is done over the entire active region. One advantage of α_w over a simple average of force-free α is that singularities at the polarity inversion lines are avoided (Tiwari et al. 2003). The weighted mean of α is

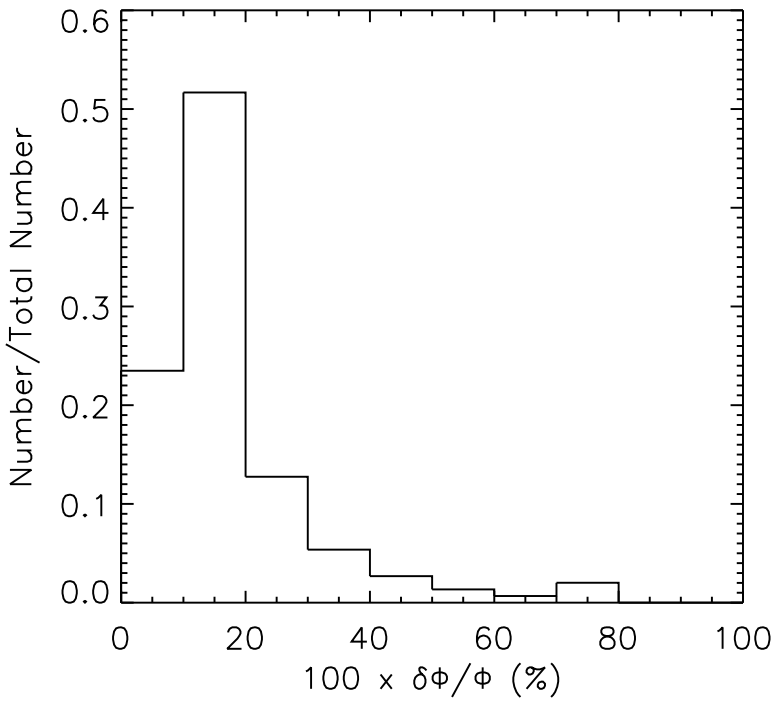

Fig. 1.— Distribution of maximum change of flux for a sample of 151 ARs. Y-axis represents number of ARs in each bin divided by the total number in the sample. Φ is median of unsigned flux and $\delta\Phi$ is the maximum change in the 24 hours of observation that are used for computation.

also believed to be one of the most robust approaches in computing α (Leka & Skumanich 1999).

ARs usually tilt away from the east-west direction, forming a tilt angle with the leading polarity towards the equator. This phenomenon is known as Joy's law. Tilt angle in an AR is defined to be the angle between the local parallel of latitude and the line connecting the centroids of opposite polarities, and usually defined to be positive when counterclockwise. This way, the angle is ordinarily negative in the northern hemisphere and positive in the southern for ARs following Joy's law. If the AR is assumed to come from a flux tube initially oriented in the east-west direction at the bottom of the CZ before it rises, this tilt angle reflects the degree of writhe in the tube and has been used in previous studies as a proxy for magnetic writhe in ARs (e.g. Longcope & Klapper 1997; Pevtsov & Canfield 1999; Tian & Liu 2003; Holder et al. 2004). To compare twist with writhe in ARs, it is convenient to rescale the tilt by dividing by the separation between the centroids of the two polarities

(Canfield & Pevtsov 1998; Holder et al. 2004). A proxy of writhe W is thus,

$$W = -\frac{\theta}{d}, \tag{2}$$

where θ is tilt angle in radians and d is the separation in cm. This way, both twist (force-free α_w) and writhe (W) have the same units. The sign of the writhe is opposite under the definition of the tilt mentioned above (Longcope et al. 1998; Holder et al. 2004). We use W as a measure of magnetic writhe in ARs.

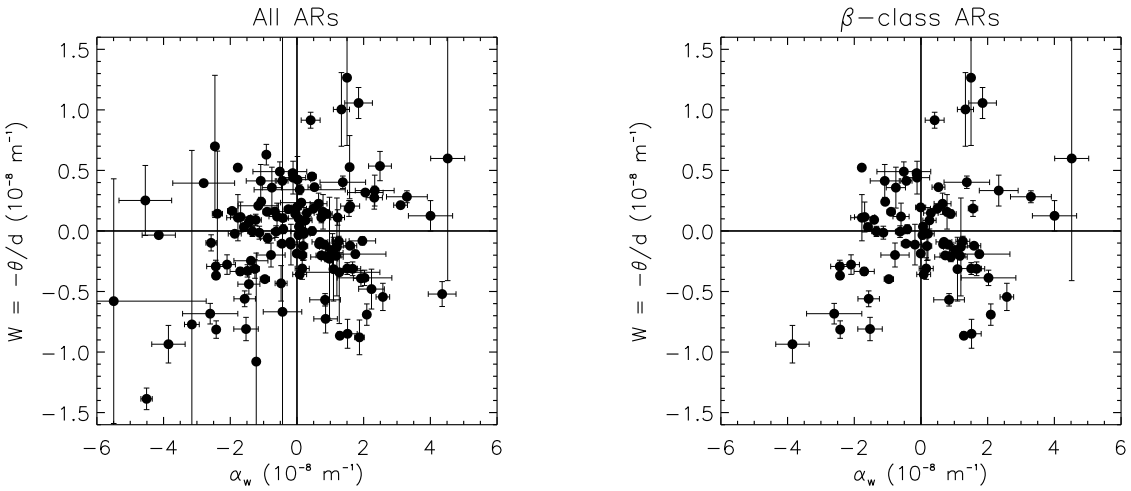

Fig. 2.— Scatter plots of α_w (X-axis) and W (Y-axis) of the sample of 151 ARs (left) and of the 82 β-class ARs. To better show the results, 21 outliers in the left panel and 6 outliers in the right are excluded in the plots.

We calculate α_w and W for each AR using observations collected during the 24 hours when the AR is closest to central meridian. Usually there are 120 datasets in this 24-hour time window. For each dataset, only pixels with field strength greater than 300 $Mx\ cm^{-2}$, roughly 3σ of field measurement (Hoeksema et al. 2013), are used for the computation. W and α_w reported here are the medians of these $\sim$120 calculations. The uncertainty in each is the standard deviations of the 120 values. Fig. 2 shows scatter plots of W and α_w for all ARs in the sample (left) and β-class ARs in the sample (right). β-class ARs, defined by Hale et al. (1919) as "a sunspot group having both positive and negative magnetic polarities (bipolar), with a simple and distinct division between the polarities," are deemed to be simple bipolar ARs, and will be analyzed separately in next Section. In the sample of 151 ARs, 76 ARs have the same signs of twist and writhe, and 75 ARs have the opposite signs. While 39 of 82 β-class ARs have the same signs and 43 have the opposite signs.

3. Results

Fig. 3 shows distributions of the sign of α_w as a function of time (X-axis) and latitude (Y-axis) for the ARs analyzed. Each dot represents one AR. Black (red) dots denote regions with positive (negative) α_w. The vertical error bar represents the standard deviation of the latitude of the AR during the 24-hour interval. The error bar in the X-axis is 24 hours wide, the time window size. From top to bottom are the sign distribution for all ARs (top), ARs having the same signs of twist and writhe (middle; $\alpha_w \cdot W > 0$; *group same* hereafter), and ARs having opposite signs of twist and writhe (bottom; $\alpha_w \cdot W < 0$; *group opposite* hereafter). The titles of the plots indicate the sample size ("AR Number") and the degree of hemispheric preference ("Yes") that refers to percentage of the ARs in the sample obeying the hemisphere rule. The fraction of the 151 ARs that follow the hemispheric rule is about 75%±7% at a 95% confidence interval. This is well within the range of the preferences for ARs reported previously in similar studies (∼58% – 82%). The sample is broken down into two groups of about the same size, 76 ARs in *group same*, and 75 ARs in *group opposite*. The percentage for *group opposite* is 87%±8%, evidently higher than that for *group same*, 64%±11%. The percentage for *group opposite* (87%) is comparable to the percentage for the quiescent filaments (∼82%) (Martin et al. 1994). It is worth noting that the ARs following the hemisphere rule in *group same* (64%) disobey Joy's law and the ARs following the hemisphere rule in *group opposite* (87%) obey Joy's law.

Tilt angle is better determined for a simple bipolar AR than for complex ARs because a simple bipolar AR has well-defined leading and following polarity patches. Based on Hale's classification (Hale et al. 1919) scheme β class AR can be deemed to be a simple bipolar AR. Each AR having β magnetic configuration when it is near the central meridian is included in the β class AR sample. Hale's classification data are from the NOAA website at $http://www.swpc.noaa.gov/ftpdir/warehouse/$. Of the 82 β-class ARs, 39 are in *group same* and 43 in *group opposite*. The results are shown in Fig. 4. 76% ± 9% of all β class ARs obey the hemisphere rule, similar to the 75% ± 7% for all 151 ARs in the sample. What is surprising is that the hemispheric preference reaches 93% (Lower and upper confidence bounds are 80% and 98% for a 95% confidence interval.)[2] for *group opposite*, showing a very strong adherence to the hemisphere rule, while only 56% ± 16% followed the rule in *group same*. The latter does not demonstrate a hemispheric preference statistically. The average amplitude of twist in both samples of all ARs and bipolar ARs does not show a dependence

[2]Using T-distribution yields a 95% confidence interval of 8%, which leads to an illogical result of upper confidence bound of 101%. A special formula based on logit transformations is thus used to calculate these asymmetric confidence limits. For references, see, e.g., $http://health.utah.gov/opha/IBIShelp/ConfInts.pdf$. The confidence intervals for the α-class ARs in Table 1 are also calculated using this method.

on solar cycle phase, consistent with previous results by Zhang et al. (2010b)

Other Hale AR classes, α class and γ/δ class, are examined and the results are listed in Table 1. The strength of the hemisphere rule in the two groups, *group same* and *group opposite*, are basically comparable for those classes of ARs. Discrepancies between the β-class ARs and other classes may be attributable to (1) smaller sample size in the other classes and (2) difficulty in determining writhe from the tilt angle in these ARs, which leads to uncertainty for dividing ARs into the two groups.

It is also worth pointing out that, in this sample of 151 ARs, the signs of α_w and mean of a partial current helicity density in the photosphere, $h_c^z = B_z(\mathbf{r})[\bigtriangledown \times \mathbf{B}(\mathbf{r})]_z$, over the whole AR are exactly the same. Here B_z is vertical component of magnetic field. Thus the hemispheric preferences of the α_w sign for different groups of ARs discovered above are also valid for the sign of h_c^z. Relationship between these two helicity proxies has also been investigated by, e.g., Hagino & Sakurai (2004); Liu & Zhang (2006); Zhang et al. (2010a).

4. Discussion and Conclusion

The purpose of this study is to test the hemisphere rule in ARs using HMI vector magnetic field data. The strength of the hemispheric preference in a sample of 151 ARs is $75\% \pm 7\%$, well within the range of the results reported in previous studies ($\sim 58\% - 82\%$). If the sample is divided into two groups based on the agreement in sign between magnetic twist and writhe, the strength in preference differs appreciably: $64\% \pm 11\%$ for the ARs having the same signs of twist and writhe and $87\% \pm 8\%$ for the ARs having opposite signs. This difference becomes even more significant in a sample of 82 ARs having a simple bipole magnetic configuration: $56\% \pm 16\%$ for the ARs having the same signs and 93% with lower and upper bounds of 80% and 98% for the ARs having the opposite signs. The strength for all 82 bipolar ARs, on the other hand, is $76\% \pm 9\%$, similar to that for the whole sample of 151 ARs.

Scenarios have been proposed to predict the sign-relationship between twist and writhe in ARs (See, e.g., Canfield & Pevtsov 1998; Pevtsov & Canfield 1999; Holder et al. 2004; Linton et al. 1996, 1999). If a flux tube originally possesses no twist, deformation of the tube during its rise through CZ due to Coriolis force (e.g., C-effect and Σ-effect) generates writhe in the tube, and at the same time generates the same amount of twist of the opposite sign to ensure conservation of helicity in the tube. In this scenario, the signs of the acquired twist and writhe are opposite, and the sign of the twist obeys the hemisphere rule (Longcope et al. 1998; Holder et al. 2004). On the other hand, if a flux tube initially has twist great

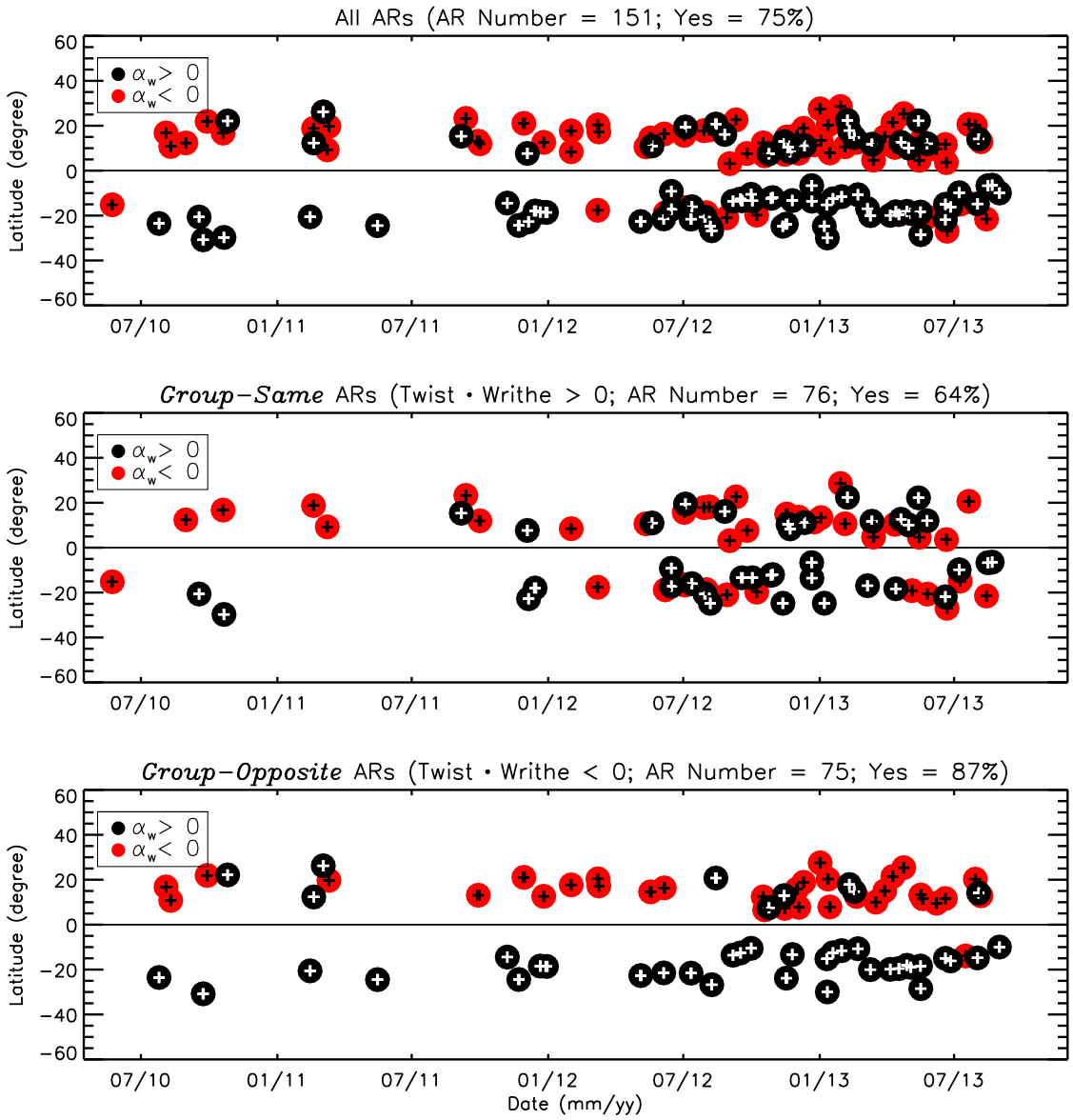

Fig. 3.— Distribution of sign of α_w in ARs as a function of latitude and time for Solar Cycle 24 from May 2010 to November 2013. "AR Number" refers to number of ARs in the sample. Percentage in the title represents how many active regions (in percentage) in the sample obey the hemisphere rule. Top panel is for all ARs; middle is for ARs having the same signs of twist and writhe; bottom is for ARs having the opposite signs of twist and writhe.

enough to lead to kink instability, part of the twist is converted to writhe. In this case, the signs of the twist and writhe are the same (Linton et al. 1996, 1999). It is not clear how this strong twist is generated in the first place. The dynamo process is one possibility.

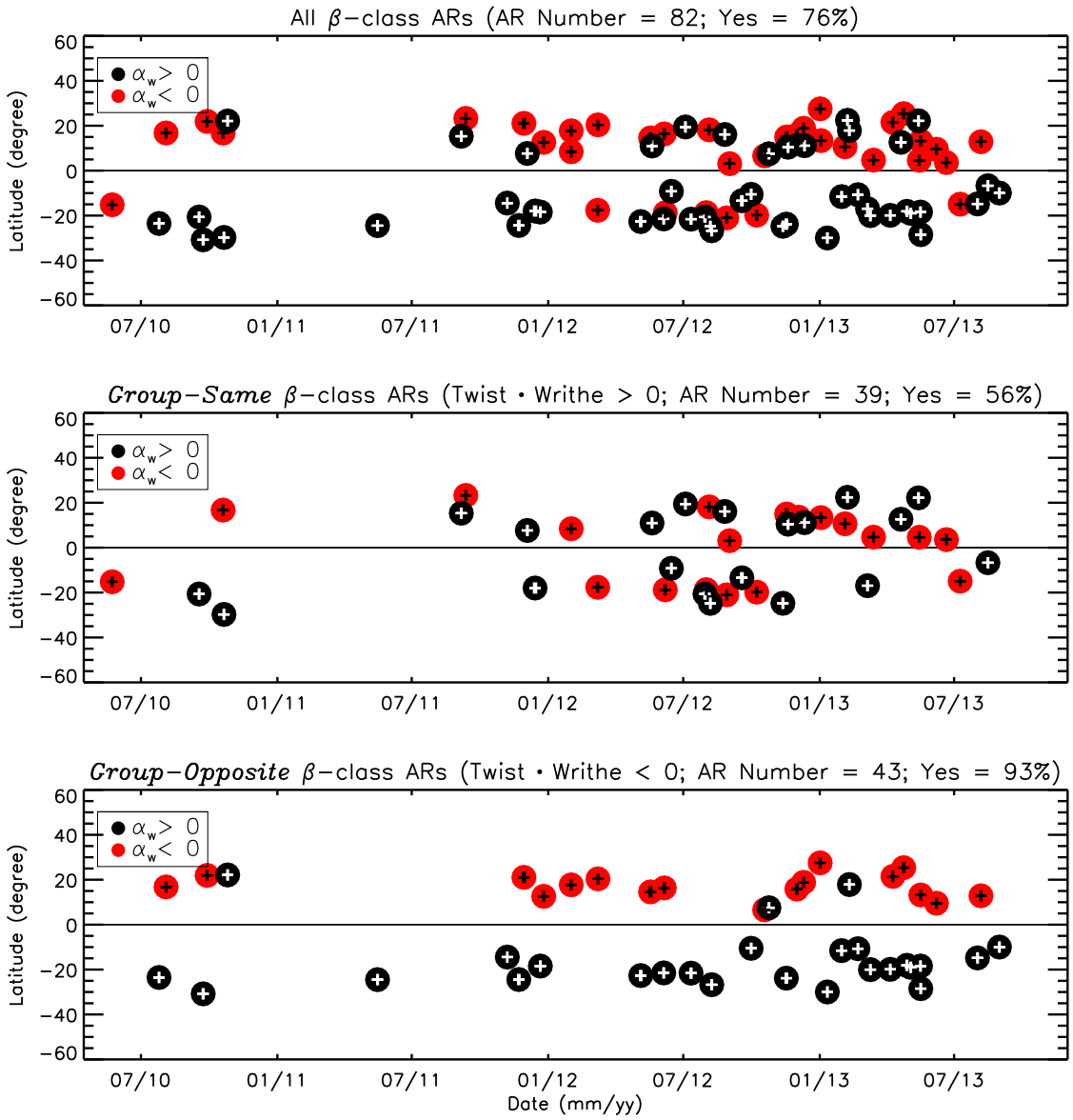

Fig. 4.— Same as Fig. 3 but only for β class ARs.

The intermediate situation, i.e., a tube that possesses twist initially but not enough to lead to kink instability, is more complicated. In this case, the relationship between the signs of the twist and writhe may depend upon which process, dynamo or emergence, plays a more important role in producing the twist. The strength of the hemisphere rule may give some indication of (1) whether or not the initial twist follows the hemisphere rule, and (2) which process is dominant, dynamo process or emergence process.

The strength of hemispheric preference differs substantially between ARs having the same signs of twist and writhe and ARs having the opposite signs. Can ARs be meaningfully divided into two groups for which the origin of magnetic twist is different? This study also shows that bipolar ARs having the same signs of twist and writhe do not have a strong hemispheric preference. Does this suggest that the twist generated by the dynamo process has no hemispheric preference? Further studies along this line would be worthwhile.

Table 1. Percentage of hemispheric preference of sign of magnetic twist for different classes of magnetic configurations of active regions.

Class of ARs[a]	Sample Size (All)	Pref.[b] (All)	Confid Bounds[c] [Lower, Upper] (All)	Sample Size ($TW < 0$)[d]	Pref. ($TW < 0$)	Confid Bounds [Lower, Upper] ($TW < 0$)	Sample Size ($TW > 0$)	Pref. ($TW > 0$)	Confid Bounds [Lower, Upper] ($TW > 0$)
All	151	75%	[68%, 82%]	75	87%	[79%, 95%]	76	64%	[53%, 75%]
α-class	24	88%	[67%, 96%]	13	85%	[51%, 97%]	11	91%	[50%, 99%]
β-class	82	76%	[67%, 85%]	43	93%	[80%, 98%]	39	56%	[40%, 72%]
γ- and/or δ-class	42	67%	[53%, 81%]	18	72%	[51%, 93%]	24	63%	[44%, 82%]

[a]Hale classification of the magnetic configuration of the AR. No Hale classification data is given for 3 ARs in this 151-AR sample.

[b]Hemisphere preference

[c]Confidence bounds are for a 95% confidence interval.

[d]$TW = \alpha_w \cdot W$.

We thank the anonymous referee for his/her comments. This work was supported by NASA Contract NAS5-02139 (HMI) to Stanford University.

REFERENCES

Abramenko, V. I., Wang. T., & Yurchishin V. B., 1996, Sol. Phys., 168, 75

Bao, S., & Zhang H., 1998, ApJ, 496, L43

Berger, M. A., & Ruzmaikin, M. A., 2000, J. Geophys. Res., 105, 10481

Bobra, M. G., X. Sun, X., Hoeksema J. T., et al., 2013, Sol. Phys., submitted

Borrero, J. H., Tomczyk, S., Kubo, M., et al., 2010, Sol. Phys., 273, 267

Brandenburg, A., Subramanian, K., Balogh, A., et al., 2011, ApJ, 734, article id. 9

Canfield, R. C., & Pevtsov, A. A., 1998, Helicity of Solar Active-Region Magnetic Fields, (ASP Conference Series), 140, 131

Centeno, R., Schou, J., Hayashi, K., et al., 2013, Sol. Phys., submitted

D'Silva, S., & Choudhuri, A. R., 1993, A&A, 272, 621

Fan, Y., Fisher, G. H., & Deluca, E. E., 1993, ApJ, 272, 621

Hagino, M., & Sakurai, T., 2004, PASJ, 56, 831

Hale G. E., Ellerman, F., Nicholson, S. B., & Joy, A. H., 1919, ApJ, 49, 153

Hao J., & Zhang, M., 2011, ApJ, 733, L27

Hoeksema, J. T., Liu, Y., Hayashi, K., et al., 2013, Sol. Phys., submitted

Holder Z. A., Canfield R. C., McMullen, R. A., et al., 2004, ApJ, 611, 1149

Kleeorin, N., Kuzanyan, K., Moss, D., et al., 2003, A&A, 409, 1097

Krause, F., & Rädler, K. H., 1980, Mean-field magnetohydrodynamics and dynamo theory (Oxford, Pergamon Press, Ltd.)

Leka K. D., Canfield R. C., McClymont, A. N., et al., 1996, ApJ, 462, 547

Leka, K. D., & Skumanich, A., 1999, Sol. Phys., 188, 3

Leka, K. D., Barnes G., Crouch, A. D., et al., 2009, Sol. Phys., 260, 83

Lim, E., & Chae, J., 2009, ApJ, 692, 104

Linton, M. G., Longcope, D. W., & Fisher, G. H., 1996, ApJ, 469, 954

Linton, M. G., Fisher, G. H., Dahlburg, R. B., & Fan, Y., 1999, ApJ, 522, 1190

Lites, B. W., Low, B. C., Martinez Pillet, et al., 1995, ApJ, 446, 877

Liu, J., & Zhang, H., 2006, Sol. Phys., 234, 1

Longcope, D. W., & Klapper, I., 1997, ApJ, 488, 443

Longcope, D. W., Fisher, G. H., & Pevtsov, A. A., 1998, ApJ, 507, 417

Martin S. F., Bilimoria, R., & Tracadas, P. W., 1994, Solar Surface Magnetism, (in NATO Advanced Science Institutes (ASI) Series C, Eds: R. J. Rutten and C. J. Schrijver. Dordrecht: Kluwer Academic Publishers), 303

Metcalf, T. R., 1994, Sol. Phys., 155, 235

Nandy, D., 2006, J. Geophys. Res., 111, CiteID A12S01

Norton, A. A., Pietarila, G. J., Ulrich, R. K., et al., 2006, Sol. Phys., 239, 69

Parker, E. N., 1955, ApJ, 122, 293

Pevtsov, A. A., Canfield, R. C. & Metcalf, T. R., 1995, ApJ, 440, L109

Pevtsov, A. A., & Canfield, R. C., 1999, Magnetic Helicity in Space and Laboratory Plasmas (AGU), 103

Pevtsov, A. A., & Balasubramaniam, K. S., 2003, *Advances in Space Research*, 32, 1867

Pouquet, A., Frisch, U., & Leorat, J., 1976, *Journal of Fluid Mechanics*, 77, 321

Rust, D. M., & Kumar, A., 1996, ApJ, 464, L199

Ruzmaikin, A. A., 1996, Geophys. Res. Lett., 23, 2649

Scherrer, P. H., Schou, J., Bush, R. I., et al., Sol. Phys., 275, 207

Schou, J., Scherrer, P. H., Bush, R. I, et al., Sol. Phys., 275, 229

Seehafer, N., 1990, Sol. Phys., 125, 219

Seehafer, N., 1996, *Physical Review E*, 53, 1283

Tian, L., & Liu, Y., 2003, A&A, 407, L13

Tiwari, S. K., Venkatakrishnan, P., Gosain, S., et al., 2009, ApJ, 700, 199

Turmon, M., Jones, H. P., Malanushenko, O. V., et al., 2010, Sol. Phys., 262, 277

Yang, S., & Zhang, H., 2012, ApJ, 758, article id. 61

Wang, Y-M, 2013, ApJ, 775, article id. L46

Zhang, H., Sokoloff, D., Rogachevskii, I., et al., 2006, MNRAS, 365, 276

Zhang, H., Yang, S., Gao, Y., et al. 2010a, ApJ, 719, 1955

Zhang, H., Sakurai, T., Pevtsov, A, et al. 2010b, MNRAS, 402, L30